Multichannel Along-Track Interferometric SAR System Implementation Using FMCW Radar

Young-Geun Kang, Seungwoon Park, Eunsung Kim, Kyeongrok Kim, and Seong-Ook Park, *Senior Member, IEEE*

***Abstract*— Along-track synthetic aperture radar interferometry (ATI) systems are used to detect a moving target and to estimate its radial velocity. A dual-channel (single-baseline) ATI system estimates the velocity ambiguously because there are many candidate velocities corresponding to the interferometric phase. To resolve the ambiguity of the estimates, a multichannel (multibaseline) ATI system is required. This letter proposes an efficient implementation technique of a multichannel ATI system by using a frequency-modulated continuous wave (FMCW) radar and an antenna arrangement method considering the inherent bi-static characteristic of FMCW radars. Also, a simple and robust radial velocity estimation algorithm suitable for the proposed system model is presented. The validity of the algorithm is confirmed with simulated ATI results.**

***Index Terms*— Along-track synthetic aperture radar interferometry (ATI), frequency-modulated continuous wave (FMCW), radial velocity estimation.**

I. Introduction

SYNTHETIC aperture radar (SAR) is a technology widely used for surveillance or terrestrial and marine observation because it generates images of large areas at any time under any weather conditions. To detect moving targets in SAR images, the along-track interferometry [1], [2] method is frequently incorporated with the SAR technique. Along-track SAR interferometry (ATI) is assessed as an efficient and practical ground-moving target indication method because of its ability to estimate the velocity of the detected moving target and low demands on the computation load.

ATI estimates the radial velocity of a moving target by measuring the phase of an interferogram generated by conjugate multiplication of SAR images formed from two channels separated by the baseline in the along-track direction. Since the phase value of a single interferogram is limited to $(-\pi, \pi]$, several velocities corresponding to the nominal ATI phase exist. Therefore, the velocity of the moving target is ambiguously estimated in a dual-channel (single-baseline) system. To resolve the ambiguity of the estimated velocity, it is necessary to introduce a multichannel ATI system and infer the actual target velocity by analyzing the estimated velocities from multiple interferograms (multibaseline) [3], [4], [5], [6], [7], [8], [9]. Because pulse radars commonly used as ATI hardware are expensive and heavy, configuring a multichannel system with pulse radars is costly and has limited options on SAR platforms. Frequency-modulated continuous wave (FMCW) radars are suitable for relatively light and compact multichannel system configurations. In fact, many attempts and studies have been conducted to implement ATI with FMCW radars [10], [11], [12].

This letter proposes an FMCW radar design and a transmit/receive antenna (T/RX) arrangement method for implementing a compact multichannel ATI system. The technique is designed for the standard mode of ATI data collection [13], considering the inherent bi-static characteristic of FMCW radars that requires TX and RX to be separated for continuous data acquisition. We also present an efficient and robust moving target velocity estimation algorithm suitable for the proposed system model. The algorithm is validated with the ATI simulated data results considering the stationary background clutter and additive thermal receiver noise to emulate the actual SAR raw data.

The rest of this letter is organized as follows. Section II derives signal models for the ATI phase and the maximum unambiguous velocity (MUV) from the FMCW radars. The proposed FMCW radar design and T/RX arrangement method to implement the multichannel ATI system are presented in Section III. Based on the MUV of the FMCW radar, a moving target velocity estimation algorithm suitable for the system is also designed. In Section IV, the algorithm is validated by presenting the velocity estimation results of a moving target. In addition, the estimation accuracy of the algorithm is confirmed by statistical estimation results. Finally, the conclusion is summarized in Section V.

II. ATI Phase and MUV of FMCW SAR

This chapter derives a complete 2-D final FMCW SAR image model of a moving target based on the signal models for FMCW SAR systems [14], [15]. This is to develop signal models for the ATI phase and the MUV from FMCW radars and to confirm whether FMCW radars produce the same result as conventional pulsed radars.

Fig. 1 shows the ATI data acquisition geometry of a moving target. x is the azimuth spatial variable, r is the slant range, $P(r_o, x_o)$ is the initial position of a moving target, v_p is the velocity of SAR platforms, v_r is the radial velocity of the moving target, and b is the baseline between two channels. The cross-range velocity of the target is assumed as zero since

Manuscript received 21 April 2023; revised 4 August 2023; accepted 17 August 2023. Date of publication 21 August 2023; date of current version 1 September 2023. *(Corresponding author: Young-Geun Kang.)*

Young-Geun Kang, Seungwoon Park, Eunsung Kim, and Seong-Ook Park are with the School of Electrical Engineering, Korea Advanced Institute of Science and Technology (KAIST), Daejeon 34141, Republic of Korea (e-mail: kbdj25@kaist.ac.kr).

Kyeongrok Kim is with the Satellite System 2 Team, Hanwha Systems, Yongin 17121, Republic of Korea.

Digital Object Identifier 10.1109/LGRS.2023.3307187

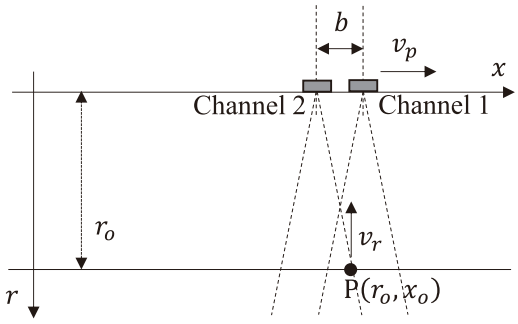

Fig. 1. ATI data acquisition geometry of a moving target.

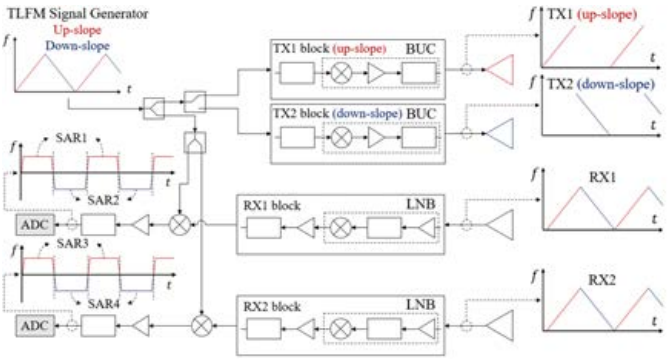

Fig. 2. Block diagram of the proposed FMCW radar design.

it has a negligible effect on the ATI phase [16]. The range between the SAR platform and the moving target is as follows:

$$r(t_a) = \sqrt{(r_o - v_r t_a)^2 + (v_p t_a - x_o)^2} \approx r_o - v_r t_a + \frac{v_p^2}{2r_o} t_a^2. \tag{1}$$

In (1), t_a is the azimuth time. Without loss of generality, x_o can be assumed as zero so that the moving target is broadside the SAR platform at $t_a = 0$. Applying the third-order Taylor series validates the approximation of (1). By incorporating this range model for the moving target into the FMCW radar signal model [14], [15] and processing with the basic range-Doppler algorithm (RDA) for FMCW SAR [17] including range deskewing [18], [19], [20], a complete 2-D FMCW SAR image model for the moving target is obtained as follows:

$$\begin{aligned} &s_{\text{out}}(f_r, t_a) \\ &= \text{sinc}\left[B_a \cdot \left(t_a - \frac{v_r}{v_p^2} r_o\right)\right] \cdot \exp\left[-j\frac{4\pi v_r}{\lambda} t_a\right] \\ &\quad \times \text{sinc}\left[T_p \cdot \left\{f_r - \frac{2}{c} k_r \cdot \left(r_o - \frac{r_o}{2} \cdot \frac{v_r^2}{v_p^2}\right)\right\}\right]. \end{aligned} \tag{2}$$

In (2), f_r is the range frequency, B_a is the Doppler bandwidth, λ is the radar wavelength, T_p is the pulse duration, and k_r is the linear chirp pulse rate. It is notable that the moving target in the FMCW SAR image is displaced by $\Delta x = v_p v_r r_o / v_p^2 = v_r r_o / v_p$ in the azimuth direction and $\Delta r = -r_o v_r^2 / (2v_p^2)$ in the range direction, respectively. The FMCW ATI phase derived from the FMCW SAR image model of a moving target is as follows:

$$\begin{aligned} \phi_{\text{ATI}} &= \phi_1(t_a) - \phi_2(t_a + \Delta t) \\ &= -\frac{4\pi v_r}{\lambda} t_a - \left(-\frac{4\pi v_r}{\lambda} \cdot (t_a + \Delta t)\right) = \frac{4\pi v_r}{\lambda} \Delta t. \end{aligned} \tag{3}$$

In (3), Δt is the short time interval between the two channels. It is shown that the FMCW ATI phase is the same as that of the pulse SAR. This implies that the ATI phase is only related to the azimuth modulation of the signal and is independent of the received range signal model (chirped or de-chirped) or the transmitted waveform. Meanwhile, since the ATI phase is limited to $(-\pi, \pi]$, the MUV of FMCW ATI is as follows, which is also the same as that of the pulse ATI:

$$\text{MUV} = \frac{\lambda}{4\Delta t}. \tag{4}$$

Note that the MUV is used as the basic parameter in the proposed moving target velocity estimation algorithm for the multichannel ATI system in Section III.

III. Multichannel FMCW ATI System Design and Velocity Estimation Algorithm

The proposed FMCW radar design for implementing a multichannel ATI system is shown in Fig. 2. Note that the proposed system is compatible with both the triangular linear frequency-modulated (TLFM) and sawtooth transmission models, but for convenience of description, it is introduced based on the TLFM model to refer to each transmitted signal clearly. As shown in Fig. 2, a TLFM signal generator and a radio frequency (RF) switch are used to implement two transmission signal sources. In addition, the TX and RX are separated since it is impossible to transmit/receive signals with a single antenna in the FMCW radar. This is the inherent bi-static characteristic of FMCW radars. The RF switch in the radar uses a square wave to split the TLFM signal into up- and down-slope parts. The two TXs alternatively transmit up- and down-slope signals and the two RXs receive the TLFM signal, respectively. Each receiver generates two SAR images by dividing the received signal into up- and down-slope signals. The proposed FMCW radar model is efficient in that it implements four channels (four SAR images) with only a single baseband signal generator and two receivers.

It is well known that an ATI system with four phase centers positioned to implement both short and long baselines is capable of accurate velocity estimation for both slow and fast objects. It is also well known that the SAR image obtained with this bi-static operation using two separated antennas is equivalent to the SAR image obtained with a single antenna, which is assumed to be located in the middle between the two antennas [21]. Considering these facts, by properly arranging the two TXs and two RXs in the along-track direction, an efficient multichannel ATI system with four equivalent phase centers can be implemented, as shown in Fig. 3. It is noteworthy that the TX2 is located at a delayed position relative to TX1 in the along-track direction. This is to generate additional phase centers by implementing the basic measurement principle of ATI. X_0 and b are key variables that determine baselines between equivalent channels and should be designed to implement both short and long baselines.

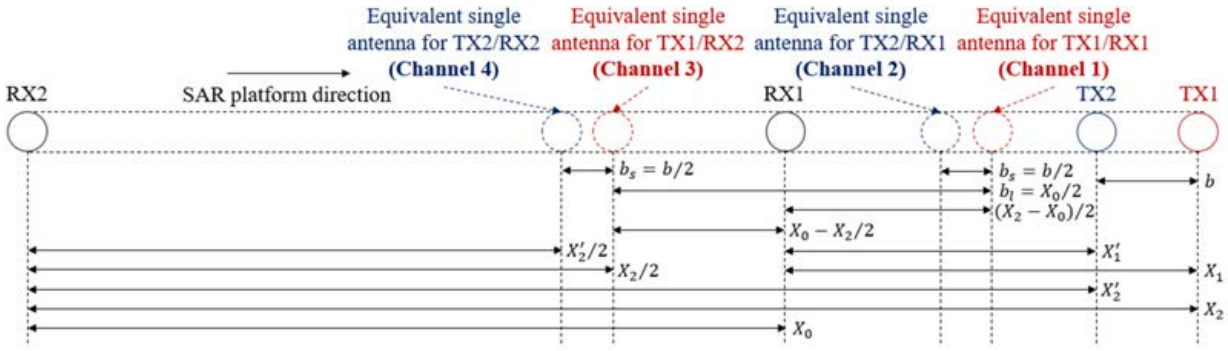

Fig. 3. Proposed T/RX arrangement method. The solid circles represent the actual positions of the T/RXs, and the dashed circles represent the positions of the virtual transceiver antennas that form the equivalent model of the real case. X_0 is the distance between the two RXs, X_1 is the distance between the RX1 and TX for the up-slope signal (TX1), X_1' is the distance between the RX1 and TX antenna for the down-slope signal (TX2), X_2 is the distance between the RX2 and TX1, X_2' is the distance between RX2 and TX2, b is the distance between the two TXs, b_s is the effective baseline between channel 1 and channel 2, and b_l is the effective baseline between channels 1 and 3.

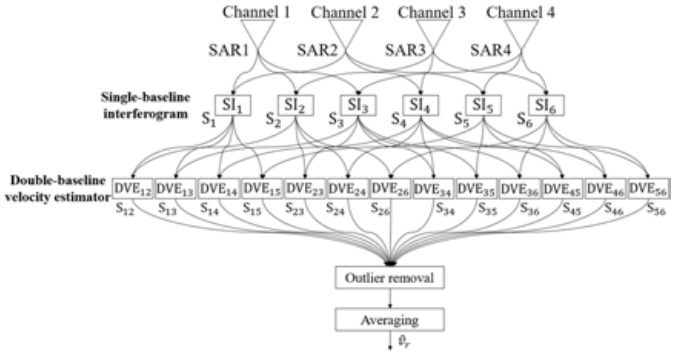

Fig. 4. Flowchart of velocity estimation algorithm for the proposed system. $\hat{v}_r$ is the estimated radial velocity of a moving target.

In addition, X_0 and b have to be designed such that the aft channel aligns with the fore channel, that is, the phase center is in the same azimuth position within a short time interval. For channel (CH) 3 to be aligned with CH1, the time interval between the two channels needs to be a multiple of pulse repetition interval (PRI)

$$\Delta t_l = \frac{b_l}{v_p} = \frac{X_0}{2v_p} = n \cdot \text{PRI} \Rightarrow X_0 = 2n \cdot v_p \cdot \text{PRI}, \quad \text{with } n = 1, 2, 3, \ldots \tag{5}$$

On the other hand, it should be noted that the time interval between CH1 and CH2 is as follows because the down-slope signal is internally delayed by half of the PRI compared to the up-slope:

$$\Delta t_s = \frac{b_s}{v_p} = \frac{b}{2v_p} = \left(m + \frac{1}{2}\right) \cdot \text{PRI} \Rightarrow b = (2m+1) \cdot v_p \cdot \text{PRI}, \quad \text{with } m = 0, 1, 2, \ldots \tag{6}$$

Although these conditions are alleviated since alignment between channels can be performed by modern signal processing techniques such as interpolation or resampling, they are strongly recommended because the clutter coherence coefficient between SAR images is assumed as 1 under these conditions [22].

A flowchart of a simple and robust velocity estimation algorithm suitable for the proposed quasi-four-channel FMCW ATI system is given in Fig. 4. In the single-baseline interferogram (SI) step, six different along-track interferograms are generated from four channels. The notation and MUV values for each SI are listed in Table I. The SI ambiguously estimates the velocity of a moving target because there are many "candidate" velocities corresponding to the measured ATI phase. The set of candidate velocities from SI_x is as follows:

$$\text{S}_x = \{2 \cdot \text{MUV}_x \cdot i + v_r \mid i \in \mathbb{Z}\} \tag{7}$$

where MUV_x is the MUV of SI_x and $\mathbb{Z}$ is the set of integers. The ambiguity can be suppressed by considering another ATI phase measured from another SI with a different baseline value. This is because only the intersection components of the two candidate velocity set corresponding to each ATI phase remain. In the double-baseline velocity estimator (DVE) step, DVE_{xy} obtains the intersection of S_x and S_y as follows:

$$\text{S}_{xy} = \text{S}_x \cap \text{S}_y = \{2 \cdot \text{IMUV}_{xy} \cdot i + v_r \mid i \in \mathbb{Z}\} \tag{8}$$

where $\text{IMUV}_{xy} = n_x \cdot \text{MUV}_x = n_y \cdot \text{MUV}_y$ is the increased MUV of DVE_{xy} where n_x and n_y are minimum natural numbers that satisfies the following equation:

$$\frac{\text{MUV}_x}{\text{MUV}_y} = \frac{n_y}{n_x}. \tag{9}$$

Although DVE also has an infinite number of candidate velocities theoretically, practical candidate velocities are limited because of the large IMUV value. This is because a moving target with a large v_r/v_p ratio is not compressed in the SAR image because of its large Doppler shift. Note that, even though there are several DVEs with the same IMUV value, the estimates are different because baselines are formed from different channels. As shown in Fig. 4, results of DVE_{16} and DVE_{25} are excluded because the two interferograms have the same baseline (MUV) value. On the other hand, even if the

TABLE I
SIX SINGLE-BASELINE INTERFEROGRAMS

	Single-baseline	MUV
$\text{SI}_1(\text{SI}_6)$	CH1-CH2 (CH3-CH4)	$\lambda/(4\Delta t_s)$
$\text{SI}_2(\text{SI}_5)$	CH1-CH3 (CH2-CH4)	$\lambda/(4\Delta t_l)$
SI_3	CH1-CH4	$\lambda/(4(\Delta t_l + \Delta t_s))$
SI_4	CH2-CH3	$\lambda/(4(\Delta t_l - \Delta t_s))$

TABLE II
ATI SIMULATION PARAMETERS

Parameter	Value
Radar frequency	10.00 GHz
System PRI	2 ms
Platform Velocity	100 m/s
X_0	2 m
b	0.6 m
MUV_1	2.50 m/s
MUV_2	0.75 m/s
MUV_3	0.58 m/s
MUV_4	1.07 m/s

ambiguity is reduced in the DVE step, in the realistic case where clutter and noise signals are present, the phase wraps even when the velocity of the moving target is near the MUV, resulting in many ambiguity estimates.

To completely disambiguate the estimate, the outlier removal and averaging processes, which have negligible computation load, are performed in turn. Even if some of the DVE results fail to accurately estimate the velocity (ambiguous estimates or outlier estimates), the algorithm is robust because there are 13 individual estimates. The process of removing outliers from the 13 estimates and averaging the remaining values accurately estimates the velocity of the moving target. In addition, the averaging process has the advantage of reducing the standard deviation of the estimated velocity to a certain degree.

IV. ATI SIMULATION RESULTS

This chapter proves the validity of the proposed FMCW ATI system and its velocity estimation algorithm by presenting the velocity estimation results with simulated ATI results of a moving target. The simulation parameters are listed in Table II. X_0 and b are set by (8) and (9). Note that because the algorithm is based on along-track interferogram results, it is recommended to maintain the prescribed platform velocity to align channels precisely. However, simple signal processing is sufficient to compensate for channel misalignments caused by deviated velocities. Stationary background clutter and additive thermal receive noise signals are added to emulate the actual SAR raw data [16]. Fig. 5 shows the process of the SAR image generation and the moving target detection in a given data acquisition geometry where a single stationary target and various moving targets exist. As shown in the last step, only the moving targets are present in the detection result images. The RDA is used to compress the SAR signal, and the method of [23] is used to detect the moving targets.

The velocity estimation was performed with the proposed algorithm while increasing the velocity of the moving target from -4 to 4 m/s by 0.01 m/s (801 estimates). As shown in Fig. 6, the SI estimation values are wrapped when the moving target velocity reaches the MUV values. Although the DVE

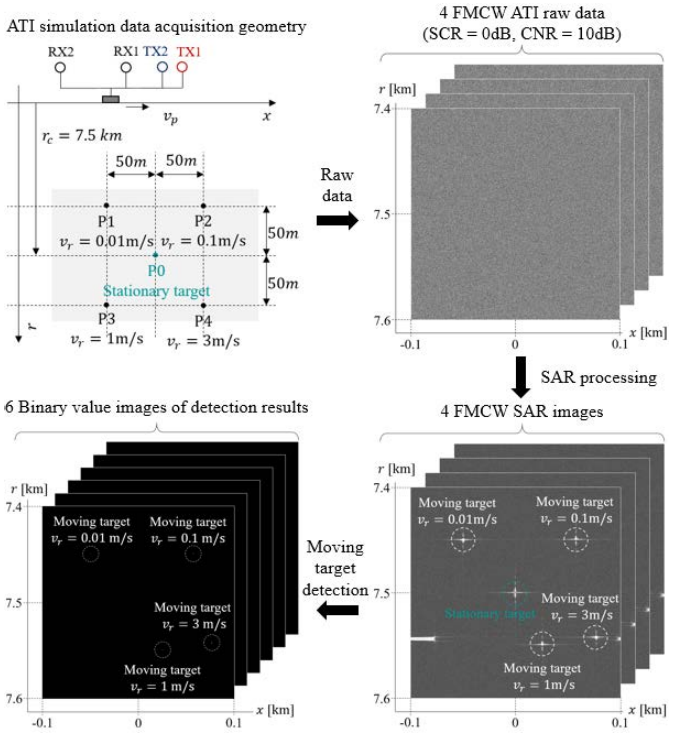

Fig. 5. Preprocessing steps of the proposed velocity estimation algorithm.

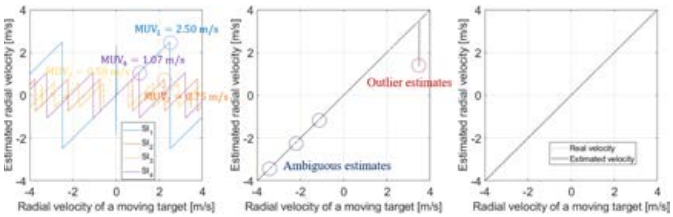

Fig. 6. Velocity estimation results of the moving target. The estimate is forced to none if it is ambiguous. (a) SI (SI_5 and SI_6 are omitted). (b) DVE_{34}. (c) Proposed method.

usually accurately estimates the velocity of the moving target, there are still many ambiguous estimates, and an outlier is also observed. The average number of ambiguous estimates found in the 13 individual DVEs was 49. This implies that DVE still suffers from ambiguity. The proposed method almost perfectly estimated the moving target velocity without a single ambiguous estimation.

To confirm the estimation accuracy of the proposed method, the velocity estimation process was repeated 1000 times to obtain statistical results of the estimation. The results for various velocities are shown in Fig. 7. The results of the proposed method have reduced standard deviations by about 36% because of the averaging process. On the other hand, the means of the estimated velocities are slightly smaller than the actual velocities. This is because the velocity is usually underestimated since the clutter signal distorts the ATI phases of the moving target signal, causing it to be biased toward zero [21]. It is also notable that SI fails to estimate a velocity

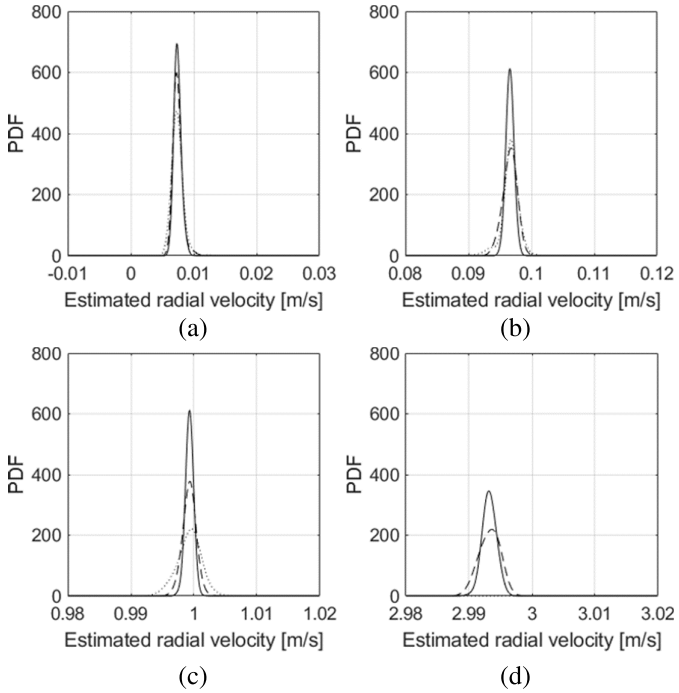

Fig. 7. Statistical estimation results for various velocities. SI (dotted line), DVE (dashed line), Proposed method (solid line). (a) 0.01 m/s. (b) 0.1 m/s. (c) 1 m/s. (d) 3 m/s.

of 3 m/s because there is no SI that can estimate a velocity above 2.5 m/s in the given ATI simulation parameters.

V. Conclusion

This letter proposed an efficient implementation of a multichannel ATI system by integrating an FMCW radar with a proper T/RX arrangement method. Compared to other pulsed multichannel ATI systems, the proposed system is expected to be inexpensive and free from platform restriction due to its lightweight and simple configuration. The proposed system is innovative in that it implements four channels with only a single baseband signal generator and two receivers. In addition, because the four channels implement short and long baselines simultaneously, the system can estimate the velocities of both slow- and fast-moving targets. An efficient and robust velocity estimation algorithm suitable for the proposed system was developed and validated the algorithm by the multichannel FMCW ATI simulations. The algorithm resolves the ambiguity of the estimated velocity by utilizing multiple along-track interferograms and enables the estimation of velocities exceeding the MUV corresponding to the shortest baseline.

Future work includes the actual implementation of the proposed system and the estimation of the actual moving object velocity using the proposed velocity estimation algorithm.

Acknowledgment

This work was supported by the Grant-in-Aid of Hanwha Systems.

References

[1] R. M. Goldstein and H. A. Zebker, "Interferometric radar measurement of ocean surface currents," *Nature*, vol. 328, pp. 707–709, Aug. 1987.

[2] R. M. Goldstein, T. P. Barnett, and H. A. Zebker, "Remote sensing of ocean currents," *Science*, vol. 246, no. 4935, pp. 1282–1285, 1989.

[3] J. H. G. Ender, P. Berens, A. R. Brenner, L. Rossing, and U. Skupin, "Multi-channel SAR/MTI system development at FGAN: From AER to PAMIR," in *Proc. IEEE Int. Geosci. Remote Sens. Symp.*, vol. 3, Toronto, ON, Canada, Jun. 2002, pp. 1697–1701.

[4] B. Himed and M. Soumekh, "Synthetic aperture radar-moving target indicator processing of multi-channel airborne radar measurement data," *IEE Proc., Radar, Sonar Navigat.*, vol. 153, no. 6, pp. 532–543, Dec. 2006.

[5] B. Friedlander and B. Porat, "VSAR: A high resolution radar system for detection of moving targets," *IEE Proc., Radar, Sonar Navigat.*, vol. 144, no. 4, pp. 205–218, Aug. 1997.

[6] B. Friedlander and B. Porat, "VSAR: A high resolution radar system for ocean imaging," *IEEE Trans. Aerosp. Electron. Syst.*, vol. 34, no. 3, pp. 755–776, Jul. 1998.

[7] M. Sletten, S. Menk, J. Toporkov, R. W. Jansen, and L. Rosenberg, "The NRL multi aperture SAR system," in *Proc. IEEE Radar Conf. (RadarCon)*, Arlington, VA, USA, 2015, pp. 192–197.

[8] M. A. Sletten, L. Rosenberg, S. Menk, J. V. Toporkov, and R. W. Jansen, "Maritime signature correction with the NRL multichannel SAR," *IEEE Trans. Geosci. Remote Sens.*, vol. 54, no. 11, pp. 6783–6790, Nov. 2016.

[9] R. W. Jansen, R. G. Raj, L. Rosenberg, and M. A. Sletten, "Practical multichannel SAR imaging in the maritime environment," *IEEE Trans. Geosci. Remote Sens.*, vol. 56, no. 7, pp. 4025–4036, Jul. 2018.

[10] G. Farquharson, H. Deng, Y. Goncharenko, and J. Mower, "Measurements of the nearshore ocean with FMCW ATI SAR," in *Proc. 10th Eur. Conf. Synth. Aperture Radar (EUSAR)*, Berlin, Germany, 2014, pp. 1–4.

[11] H. Deng, G. Farquharson, J. Sahr, Y. Goncharenko, and J. Mower, "Phase calibration of an along-track interferometric FMCW SAR," *IEEE Trans. Geosci. Remote Sens.*, vol. 56, no. 8, pp. 4876–4886, Aug. 2018.

[12] S. An, D.-J. Kim, J.-H. Hwang, and J. Song, "Implementation of ATI-GMTI process on airborne and automobile SAR data," in *Proc. 7th Asia–Pacific Conf. Synth. Aperture Radar (APSAR)*, Bali, Indonesia, 2021, pp. 1–5.

[13] Y. Zhang, "Along track interferometry synthetic aperture radar (ATI-SAR) techniques for ground moving target detection," Defense Tech. Inf. Center, Fort Belvoir, VA, USA, Tech. Rep. AFRL-SN-RS-TR-2005-410, Jan. 2006.

[14] A. Meta, P. Hoogeboom, and L. P. Ligthart, "Signal processing for FMCW SAR," *IEEE Trans. Geosci. Remote Sens.*, vol. 45, no. 11, pp. 3519–3532, Nov. 2007.

[15] Y. Liu, Y. K. Deng, R. Wang, and O. Loffeld, "Bistatic FMCW SAR signal model and imaging approach," *IEEE Trans. Aerosp. Electron. Syst.*, vol. 49, no. 3, pp. 2017–2028, Jul. 2013.

[16] A. Budillon, V. Pascazio, and G. Schirinzi, "Estimation of radial velocity of moving targets by along-track interferometric SAR systems," *IEEE Geosci. Remote Sens. Lett.*, vol. 5, no. 3, pp. 349–353, Jul. 2008.

[17] Y.-G. Kang, D.-H. Jung, G.-H. Shin, C.-K. Kim, and S.-O. Park, "A Study on the feasibility of stop-and-go approximation in FMCW SAR," *J. Electromagn. Eng. Sci.*, vol. 22, no. 3, pp. 210–217, May 2022.

[18] A. Ribalta, "Time-domain reconstruction algorithms for FMCW-SAR," *IEEE Geosci. Remote Sens. Lett.*, vol. 8, no. 3, pp. 396–400, May 2011.

[19] C. Stringham and D. G. Long, "GPU processing for UAS-based LFM-CW stripmap SAR," *Photogramm. Eng. Remote Sens.*, vol. 80, no. 12, pp. 1107–1115, 2014.

[20] W. G. Carrara, R. S. Goodman, and R. M. Majewski, *Spotlight Synthetic Aperture Radar*. Boston, MA, USA: Artech House, 1995.

[21] S. V. Baumgartner and G. Krieger, "Multi-channel SAR for ground moving target indication," in *Academic Press Library in Signal Processing*, vol. 2. Amsterdam, The Netherlands: Elsevier, 2014, pp. 911–986.

[22] C. W. Chen, "Performance assessment of along-track interferometry for detecting ground moving targets," in *Proc. IEEE Radar Conf.*, Philadelphia, PA, USA, Apr. 2004, pp. 99–104.

[23] G. Gao and G. Shi, "The CFAR detection of ground moving targets based on a joint metric of SAR interferogram's magnitude and phase," *IEEE Trans. Geosci. Remote Sens.*, vol. 50, no. 9, pp. 3618–3624, Sep. 2012.